



Effect of forced cooling on the tensile properties and impact toughness of the coarse-grained heat-affected zone of a high-strength structural steel

Juhani Laitila¹ · Jari Larkiola¹ · David Porter¹

Received: 10 July 2017 / Accepted: 18 November 2017 / Published online: 5 December 2017
© International Institute of Welding 2017

Abstract

The effects of forced cooling, i.e., forced cooling rate and forced cooling finish temperature, on the tensile and impact toughness properties of simulated weld coarse-grained heat-affected zones has been explored in the case of a low-carbon thermomechanically processed steel with a yield strength of 700 MPa. The forced cooling finish temperatures that were studied were 400, 300, 200, and 100 °C and the forced cooling rates were 50 and 15 °C/s. Coarse-grained heat-affected zones were simulated using a Gleeble 3800 thermomechanical simulator. For the steel concerned, strength and impact toughness improved significantly when the steel was cooled rapidly to 200 or 100 °C. The results indicate that it may be possible to substantially improve welding productivity by using forced cooling to reduce interpass times.

Keywords Bainite · Cooling rate · Coarse-grained heat-affected zone · High-strength steels · Welding

1 Introduction

High-strength steels are becoming more commonly used in the engineering and construction industry. By using high-strength structural steels, the structures can be made lighter and more elegant due to thinner wall thicknesses. Furthermore, the financial burden of structural projects can be eased with high-strength steels due to lower overall material costs. However, production time is usually greatly increased because of the need to use more welding passes when high-strength steels are used compared to normal structural steels such as S355 [1–3].

Multipass welding is usually used to achieve sufficiently narrow heat-affected zones and sufficiently high cooling rates.

The cooling rate has a significant impact on the mechanical properties of the welded joint because it controls the microstructural changes that occur in the steel during welding. Usually steel manufacturers provide recommended weld cooling times between 800 and 500 °C (t_{8/5}) along with recommendations about interpass temperatures and heat inputs. The higher the strength the shorter the recommended maximum t_{8/5} time tends to be in order to achieve welds with sufficiently high strength.

In addition, steel producers often provide guidelines for the number of weld passes that should be used to achieve the desired cooling time. For example, SSAB recommends the use of three weld passes for Strenx high-strength steels when the material thickness is between 6 and 8 mm [4]. The required number of weld passes increases as the material thickness increases. This means increased production times due to the time spent waiting for the steel to cool down to the recommended interpass temperature.

Recommended interpass temperatures are around 200–300 °C when high-strength structural steels are used [4–7]. In some cases it can be as high as 400 °C. However, when higher interpass temperature is used, lower heat input is required to avoid exceeding the maximum allowed value of t_{8/5}, which can be counterproductive by leading to the need for additional weld beads. Furthermore, usually with higher

Recommended for publication by Commission IX - Behavior of Metals Subjected to Welding

✉ Juhani Laitila
Juhani.Laitila@Oulu.fi

Jari Larkiola
Jari.Larkiola@Oulu.fi

David Porter
David.Porter@Oulu.fi

¹ Materials and Production Engineering, Faculty of Technology, University of Oulu, Pentti Kaiteran Katu 1, 90570 Oulu, Finland

interpass temperature, the heat-affected zone is wider and the allowed heat input is lower, which again increases the number of weld passes required.

Ideally, from a productivity point of view, external cooling should be introduced when welding high-strength steel. This would enable the steel to reach the interpass temperature faster. Furthermore, external cooling would allow an increased heat input and the number of weld passes to be reduced. Both of these effects would increase workshop productivity by eliminating a significant amount of the time wasted in the welding process due to waiting in between the weld passes.

It is known that high-strength steels that consist of bainite, martensite, or a mixture of the two undergo microstructural changes in temperatures below 500 °C [8]. However, the traditional $t_8/5$ has been uniformly used in welding specifications regardless of the material for decades. While it may have been a suitable parameter in the past, with high-strength steels becoming more common, it may no longer be the optimal choice. Instead, the formulation of a new index might be more appropriate and even allow an increase in the productivity of welded high-strength steel structures. It is also proposed in this paper that a new cooling index that measures the time between 800 °C and the interpass temperature should be used along with the external forced cooling in order to maximize productivity. The reason for this is that microstructural changes still occur between 500 °C and the interpass temperature.

In a previous study conducted by Hoy et al. (2015), it was discovered that six different low-carbon steels became brittle when they were cooled down to below 300 °C rapidly [9]. Steels react differently to cooling cycles due to changes in alloying elements and therefore, it is necessary to establish cooling cycles individually for each steel. Apart from production time considerations, rapidly cooling the steel to temperatures below 500 °C has the potential to produce lower bainite in the weld joint and thereby improve the strength, toughness, and elongation to fracture of the joint. Lower bainite is able to have similar strength to that of martensite while having better toughness and elongation, making it the ideal microstructure in the heat-affected zone (HAZ) [10].

Usually in high-strength steel welds, the areas with the lowest strength and lowest toughness are located in the HAZ. In this zone, the base material has not melted, but has undergone microstructural changes because of the thermal cycle imposed on the steel by the heat produced by the welding process. The HAZ can be divided into four main sub-categories: coarse-grained (CGHAZ), fine-grained (FGHAZ), intercritical (ICHAZ), and subcritical (SCHAZ). These areas are produced by different peak temperatures in the weld. In the case of multipass welding, the CGHAZ of an earlier pass can be heated into the intercritical temperature region by a later pass producing an intercritically reheated CGHAZ (ICCGHAZ). The CGHAZ can usually be produced with peak temperature of 1350 °C, while the SCHAZ on the

other side of the spectrum can be produced for example, with peak temperature of 600 °C. Regarding tensile strength, the weakest zones tend to be the SCHAZ or ICHAZ [11, 12]. Regarding fracture toughness, the lowest toughness regions can be the ICCGHAZ, the CGHAZ, or the ICHAZ depending on the steel composition. These are known as local brittle zones (LBZ). By reducing the required number of weld passes, the incidence of these zones is reduced and the risk of fracture in the joint is thereby lowered [13].

This research paper focuses on the effect of the forced cooling finish temperature (FCFT) and forced cooling rate on the mechanical properties of the CGHAZ due to the fact that it is usually an area with low toughness in welded joints. If the steel can be forcibly cooled at high speeds directly to the interpass temperature without loss of mechanical properties, significant amounts of time can be saved in the welding process. By eliminating wasted time, the attractiveness of high-strength structural steels to the construction industry can be increased leading to their wider application.

2 Experimental procedures

The experimental part of the research was based on simulated CGHAZs forced cooled to low temperatures using a Gleeble thermomechanical simulator. The mechanical properties of the CGHAZs were evaluated as regards tensile properties and impact toughness.

The material used in the tests was a 6 mm thick commercial grade high-strength steel. The material was chosen due to its suitability for the construction industry and the fact that it has a mainly bainitic microstructure [14]. The steel has a minimum specified yield strength ($R_{p0.2}$) of 700 MPa, a tensile strength (R_m) in the range 750–950 MPa, an elongation to fracture (A) of at least 13% and a specified minimum impact strength of 27 J at –40 °C. The chemical composition of the steel as given by the manufacturer is shown in Table 1.

The recommended cooling time $t_8/5$ for this steel is from 5 to 20 s. However, if matching weld strength is desired, $t_8/5$ should be ≤ 10 s, according to the manufacturer [4]. The steel has a typical carbon equivalent (CEV) of 0.37 which is associated with good weldability. ($CEV = C + Mn/6 + (Cu + Ni)/15 + (Cr + Mo + V)/5$, where the symbols represent the steel alloy content in wt.%) [15].

The test specimens used in the Gleeble tests were cut in longitudinal direction of rolled plates and had the dimension

Table 1 Chemical composition of the steel, wt.% [15]

C max	Si max	Mn max	P max	S max	Al min.
0.10	0.20	2.10	0.020	0.010	0.015

Table 2 Simulated air cooling rates

Temperature range (°C)	Cooling rate (°C/s)
500–450	7.10
450–400	5.00
400–350	3.85
350–300	2.77
300–250	2.00
250–200	1.28
200–150	0.69
150–100	0.29

of $10 \times 5 \times 55$ mm and $120 \times \text{Ø}6$ mm. The specimens were cut from plates by using water jet cutting to avoid heating of the steel. After the cutting, samples were machined to fulfill the required tolerance of the standard ISO 148-1 for the Charpy V-notch specimens, excluding the notch. The notches for the Charpy V-notch tests were machined after the Gleeble simulation. Testing was carried out at -40 °C. After testing, ductile fracture percentages were evaluated according to ISO 148-1.

The tensile test specimens were also machined to their final dimension after the Gleeble simulation. Before the simulations, the specimens had dimension of $120 \times \text{Ø}6$ mm. After the Gleeble simulation, the tensile specimens were machined to have a parallel length of 15 mm and a nominal diameter of 4 mm. The gauge length of the specimens was 10 mm. Tensile tests were carried out with a Zwick 100kN testing machine.

A Gleeble 3800 was used to impose thermal cycles on the steel to simulate the CGHAZs that might be produced by enhancing the cooling rate of welds down to different temperatures followed by cooling in still air. A peak temperature of

1350 °C was chosen to promote rapid austenite grain growth resulting in a CGHAZ with a low impact and fracture toughness [16, 17]. The specimens were heated to 1350 °C at 400 °C/s where they were held for 1 s before rapid cooling at 50 or 15 °C/s. The rapid cooling stage was terminated at different temperatures, i.e., 500, 400, 300, 200, and 100 °C, after which cooling was continued following the rates given in Table 2, which are representative of the free cooling of a weld in air. Figure 1 shows examples of two thermal cycles, i.e., where rapid cooling was terminated at 500 or 100 °C.

The low-temperature cooling rates shown in Table 2 were derived from measurements on a T-joint welded between square structural hollow sections with the dimensions $150 \times 150 \times 8$ mm and $100 \times 100 \times 8$ mm with a 5-mm fillet weld using a heat input of 1.5 kJ/mm. The temperature of the weld was measured down to 100 °C and formed the basis for the cooling data shown in Table 2. It is worth noting that the measured cooling times were significantly different to times calculated according to the Rosenthal theory.

3 Results and discussion

3.1 Impact toughness

Individual absorbed energy and percentage ductile fracture values are shown in Tables 3 and 4, while mean absorbed energy values are shown in Fig. 2 and mean ductile fracture surface percentage in Fig. 3. It can be seen that when the cooling rate was 50 °C/s, the CGHAZ had similar toughness irrespective of the FCFT. However, when the cooling rate was reduced to 15 °C/s, there was significant variation between different lower limits of rapid cooling.

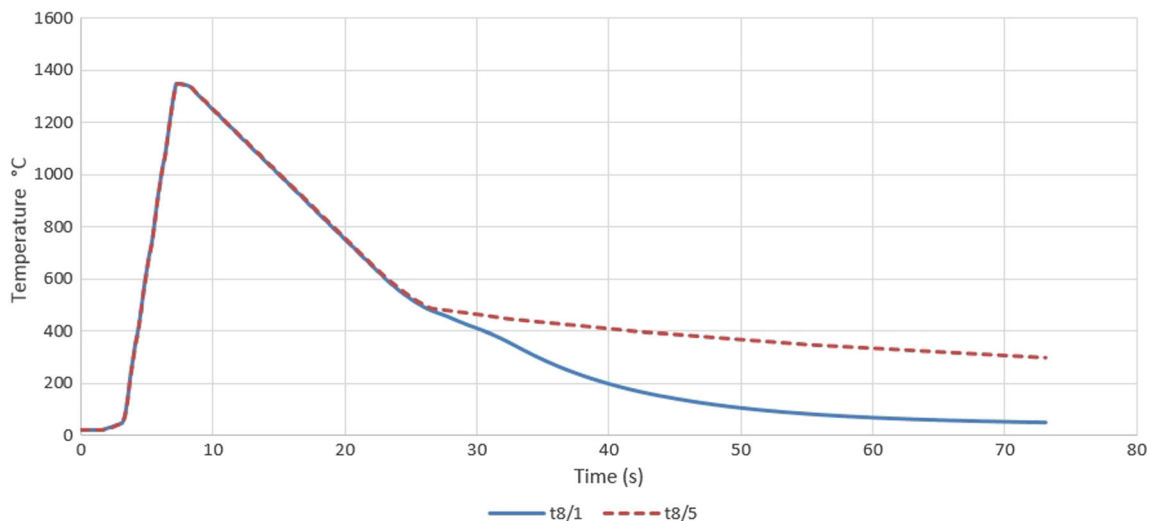
**Fig. 1** Thermal cycle with cooling rate of 50 °C

Table 3 Toughness values and percentage of ductile fracture at $-40\text{ }^{\circ}\text{C}$ for specimens cooled at $50\text{ }^{\circ}\text{C/s}$

FCFT, $^{\circ}\text{C}$	#1	#2	#3	Median
500	76 J 80%	78 J 85%	83 J 100%	78 J 85%
400	78 J 100%	82 J 100%	90 J 100%	82 J 100%
300	70 J 80%	90.5 J 90%	92 J 100%	90.5 J 90%
200	74 J 70%	75 J 75%	77.5 J 95%	75 J 75%
100	82 J 95%	82 J 100%	99.5 J 100%	82 J 100%

Table 3 shows that all of the fracture surfaces were mainly ductile with the faster cooling speed of $50\text{ }^{\circ}\text{C/s}$. Therefore, the test temperature of $-40\text{ }^{\circ}\text{C}$ is usually on or close to the upper shelf of the transition curve. The highest individual toughness level in this study was achieved with a FCFT of $100\text{ }^{\circ}\text{C}$ when the cooling speed was $50\text{ }^{\circ}\text{C/s}$.

For the slower cooling rate of $15\text{ }^{\circ}\text{C/s}$, the test temperature of $-40\text{ }^{\circ}\text{C}$ is in the ductile–brittle transition temperature range with ductile fracture percentages falling as low as 20%. Now there is a clear effect of FCFT: both absorbed energy and percentage ductile fracture show a minimum when the cooling finish temperature is $300\text{ }^{\circ}\text{C}$.

3.2 Strength

The strength of the CGHAZ was tested for different cooling rates of 50 and $15\text{ }^{\circ}\text{C/s}$. The values shown in Figs. 4 and 5 are the average values of three specimens. Figure 4 shows that for both forced cooling rates, tensile strength at room temperature

Table 4 Toughness values and percentage of ductile fracture at $-40\text{ }^{\circ}\text{C}$ for specimens cooled at $15\text{ }^{\circ}\text{C/s}$

FCFT, $^{\circ}\text{C}$	#1	#2	#3	Median
500	73 J 60%	92 J 60%	102 J 70%	92 J 60%
400	11.5 J 20%	51 J 40%	87 J 70%	51 J 40%
300	15.5 J 20%	50 J 40%	68 J 50%	50 J 40%
200	18 J 20%	66 J 50%	84 J 65%	66 J 50%
100	14 J 20%	92 J 100%	107.5 J 100%	92 J 100%

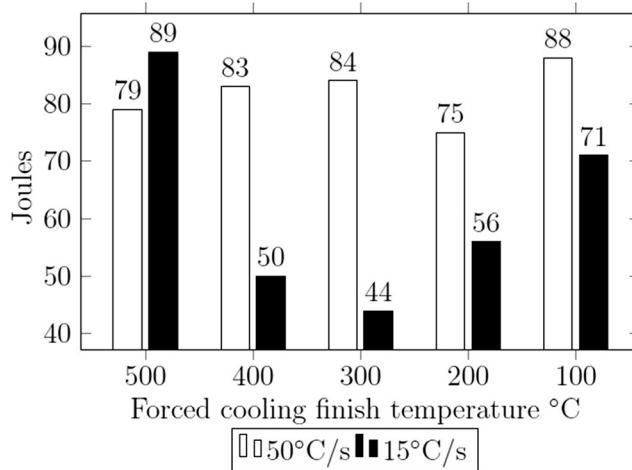


Fig. 2 Charpy V impact toughness at $-40\text{ }^{\circ}\text{C}$ for different cooling rates

increases with decreasing FCFT. However, with yield strength this was not the case when the cooling rate was $15\text{ }^{\circ}\text{C/s}$.

The increase in tensile strength was 12% between 500 and $100\text{ }^{\circ}\text{C}$ with the faster cooling speed of $50\text{ }^{\circ}\text{C/s}$ and 8% with the lower cooling rate of $15\text{ }^{\circ}\text{C/s}$. In this study, the greatest increase in tensile strength of 9.5% was observed between 500 and $200\text{ }^{\circ}\text{C}$, with cooling speed of $15\text{ }^{\circ}\text{C/s}$.

The highest yield strength values were obtained with the cooling speed of $50\text{ }^{\circ}\text{C/s}$ combined with a FCFT of $200\text{ }^{\circ}\text{C}$. With the slower cooling speed of $15\text{ }^{\circ}\text{C/s}$, the highest yield strength was obtained with a FCFT of $400\text{ }^{\circ}\text{C}$.

Overall, decreasing the FCFT to 200 or $100\text{ }^{\circ}\text{C}$ had no detrimental effect on the tensile or yield strength. Furthermore, the Y/T-ratio improved when the lower limit was below $500\text{ }^{\circ}\text{C}$, except for the case of $400\text{ }^{\circ}\text{C}$ with cooling rate of $15\text{ }^{\circ}\text{C/s}$ as can be seen in Fig. 6. The Y/T-ratio improved by 13% with lower temperature of $100\text{ }^{\circ}\text{C}$ instead of

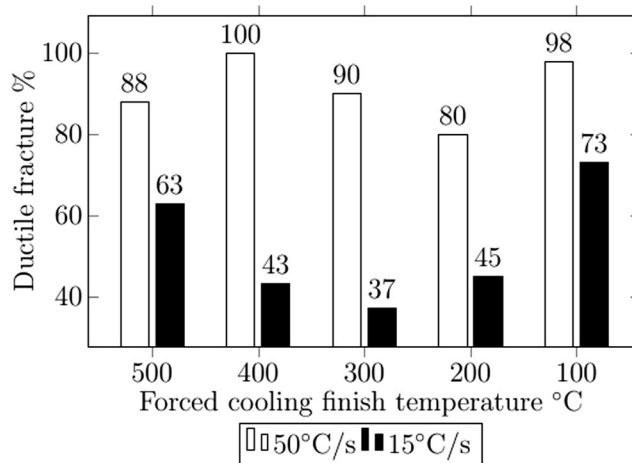


Fig. 3 Percentage of mean ductile fracture at $-40\text{ }^{\circ}\text{C}$ for different cooling rates

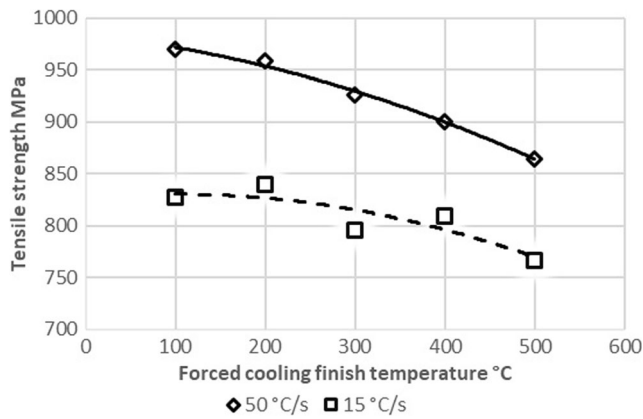


Fig. 4 Tensile strength of the CGHAZ for different cooling rates

500 °C using the cooling speed of 50 °C/s. The improvement was 5% with a cooling speed of 15 °C/s.

On the basis of these results, as the FCFT is decreased, the CGHAZ becomes more able to deform before breaking. Of course, these results only represent the contribution of the CGHAZ. If the same behavior is applicable to other regions of the HAZ, it would be beneficial to the behavior of the weld as a whole. Higher strength HAZs are able to better resist local necking by contributing to overmatching and thereby shifting deformation during cross-weld overloading towards the base material. This can be very important in various kind of structures, for example if they are located in earthquake prone areas or in danger of other accidental overloading. The beneficial effects of low FCFT on Y/T-ratio are also important in situations where stress levels above the yield strength are present: the lower the Y/T-ratio the more plastic deformation the material can tolerate [18, 19].

3.3 Uniform elongation

As shown in Fig. 7, the uniform elongation of the CGHAZ is clearly improved by reducing the FCFT to low temperatures in the region of 200–100 °C. Usually, the specimens with a lower cooling speed of 15 °C/s had better uniform elongation

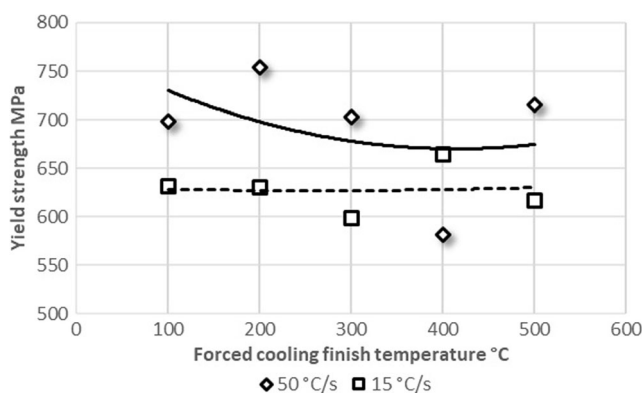


Fig. 5 Yield strength (0.2% proof stress) of the CGHAZ for different cooling rates

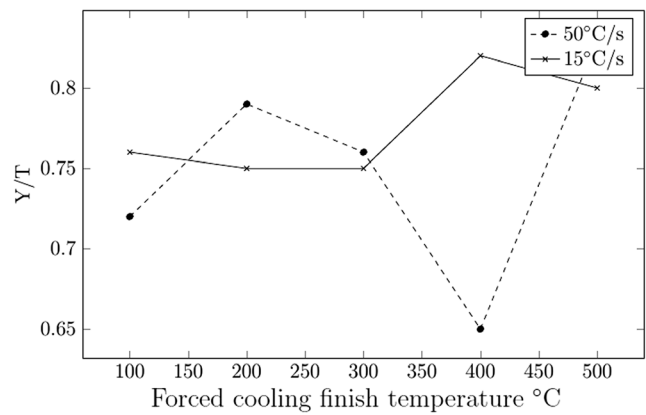


Fig. 6 Y/T ratios of the CGHAZ for different cooling rates

values than the specimens with a cooling speed of 50 °C/s. The highest elongation values were achieved with lower limit of 200 °C irrespective of the cooling speed in this study. With cooling speed of 50 °C/s, the elongation increased by 12.8% between 500 and 200 °C and by 11.6% between lower limits of 500 and 100 °C. With cooling speed of 15 °C/s, the elongation increased by 19.4% between 500 and 200 °C and by 4.4% between 500 and 100 °C.

3.4 Microstructure

Extensive microstructural investigations were not undertaken in this study. In general, mechanical properties are, of course, the result of the microstructure that results from the applied processing parameters. One example of the changes that can be brought about by the application of forced cooling to the present steel is shown in Fig. 8, which shows the microstructures of simulated CGHAZs obtained with FCFTs of 500 and 100 °C. The differences are striking, with the lower FCFT showing a much finer bainite lath thickness than the higher FCFT. This is presumably due to the fact that most of the bainite forms at temperatures below 500 °C. With forced cooling to lower temperatures, more bainite is formed at lower temperatures where the lath thickness is known to be finer

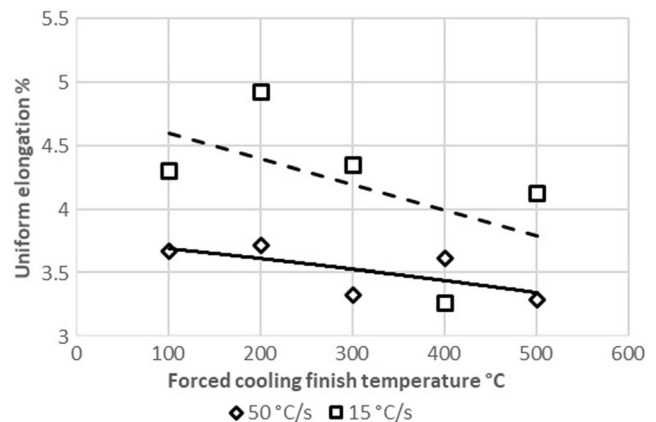
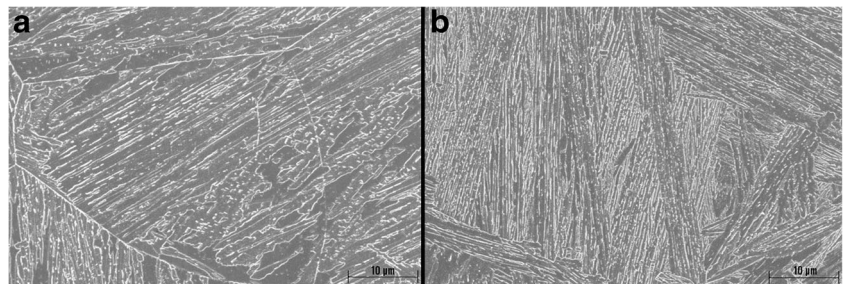


Fig. 7 Uniform elongation of CGHAZ for different cooling rates

Fig. 8 Microstructure of the simulated CGHAZ with a cooling rate of 50 °C/s. **a** FCFT 500 °C. **b** FCFT 100 °C



[20]. When simulated air cooling starts at 500 °C, more bainite will be able to grow at higher temperatures. In general finer microstructures are associated with higher strength. However, other factors being equal, higher strength will tend to raise the ductile—brittle transition temperature and lower the absorbed energy in the Charpy V test if the test temperature is in the transition temperature range. However, the finer bainite will contain finer carbides that are beneficial to toughness [21]. Transition temperature and absorbed energy are also affected by, e.g., the packet size, i.e., effective grain size of the bainitic microstructure [22]. This will depend on the details of the prior austenite grain size and how the bainite packets nucleate and grow. These aspects of the effects of forced cooling would require further investigations.

4 Conclusion

On the basis of this research concerning the strength and toughness of the CGHAZ in a high-strength thermomechanically processed steel with a yield strength of 700 MPa, it appears that, from both a productivity and a mechanical property point of view, it would be beneficial to force cool the welds in such steels down to 100 or 200 °C. There are indications that the refinement of the CGHAZ bainite lath thickness is the reason for the higher strength and impact toughness that can be achieved with a suitable cooling rate.

This has been preliminary research and the work should be continued to consider the properties of other subzones in the HAZ such as the ICHAZ and SCHAZ and to consider other low-carbon thermomechanically processed high-strength steels to establish suitable forced cooling rates and forced cooling finish temperatures.

In practice, the challenge will be the forced cooling process itself, because cooling welds down to 100 °C at a high rate is problematic with the cooling methods currently on the market.

Acknowledgements The authors acknowledge Jukka Haapio for providing the basis of the data in Table 2 by conducting the cooling time experiments on the T-joint welds at the company Kemppi Oy in Lahti, Finland. We are grateful to Juha Uusitalo of the University of Oulu for conducting the Gleeble simulations. The authors are grateful for the financial support of Tekes—the Finnish Funding Agency for Innovation within the

DIMECC program MANU—Future digital manufacturing technologies and systems.

References

1. Javidan F, Heidarpour A, Zhao X-L, Hutchinson CR, Minkinen J (2016) Effect of weld on the mechanical properties of high strength and ultra-high strength steel tubes in fabricated hybrid sections. *Eng Struct* 118:16–27. <https://doi.org/10.1016/j.engstruct.2016.03.046>.
2. Qiang X, Jiang X, Bijlaard FS, Kolstein H (2016) Mechanical properties and design recommendations of very high strength steel {960} in fire. *Eng Struct* 112:60–70. <https://doi.org/10.1016/j.engstruct.2016.01.008>
3. Romero ML, Ibaez C, Espinos A, Portols J, Hospitaler A (2016) Influence of ultra-high strength concrete on circular concrete-filled dual steel columns. *Structure*. <https://doi.org/10.1016/j.istruc.2016.07.001>.
4. NN (2016) Welding of strenx. SSAB. www.ssab.com/Products/Brands/Strenx/Products/Strenx-700-MC!tab=workshop. Accessed: 3 Feb 2016
5. Lan L, Kong X, Qiu C, Zhao D (2016) Influence of microstructural aspects on impact toughness of multi-pass submerged arc welded HSLA steel joints. *Mater Des* 90:488–498. <https://doi.org/10.1016/j.matdes.2015.10.158>
6. Wang X, Wang X, Shang C, Misra R (2016) Characterization of the multi-pass weld metal and the impact of retained austenite obtained through intercritical heat treatment on low temperature toughness. *Mater Sci Eng A* 649:282–292. <https://doi.org/10.1016/j.msea.2015.09.030>
7. Kim J, Yoon E (1998) Notch position in the HAZ specimen of reactor pressure vessel steel. *J Nucl Mater* 257(3):303–308. [https://doi.org/10.1016/S0022-3115\(98\)00451-6](https://doi.org/10.1016/S0022-3115(98)00451-6)
8. Kumar S, Nath S, Kumar V (2016) Continuous cooling transformation behavior in the weld coarse grained heat affected zone and mechanical properties of Nb-microalloyed and HY85 steels. *Mater Des* 90:177–184. <https://doi.org/10.1016/j.matdes.2015.10.071>
9. Sung HK, Lee DH, Shin SY, Lee S, Yoo JY, Hwang B (2015) Effect of finish cooling temperature on microstructure and mechanical properties of high-strength bainitic steels containing Cr, Mo, and B. *Mater Sci Eng A* 624:14–22. <https://doi.org/10.1016/j.msea.2014.11.035>
10. Samanta S, Biswas P, Giri S, Singh SB, Kundu S (2016) Formation of bainite below the MS temperature: kinetics and crystallography. *Acta Mater* 105:390–403. <https://doi.org/10.1016/j.actamat.2015.12.027>
11. Kim S, Kang D, Kim T-W, Lee J, Lee C (2011) Fatigue crack growth behavior of the simulated HAZ of 800 MPa grade high-performance steel. *Mater Sci Eng A* 528(6):2331–2338. <https://doi.org/10.1016/j.msea.2010.11.089>
12. Chen X-w, Liao B, Qiao G-Y, Gu Y, Wang X, Xiao F-R (2013) Effect of nb on mechanical properties of haz for high-nb x80

- pipeline steels. *J Iron Steel Res Int* 20(12):53–60. [https://doi.org/10.1016/S1006-706X\(13\)60216-2](https://doi.org/10.1016/S1006-706X(13)60216-2)
13. Jil Jang J, Lee B-W, Ju J-B, Kwon D, sik Kim W (2003) Experimental analysis of the practical LBZ effects on the brittle fracture performance of cryogenic steel HAZs with respect to crack arrest toughness near fusion line. *Eng Fract Mech* 70(10):1245–1257. [https://doi.org/10.1016/S0013-7944\(02\)00111-X](https://doi.org/10.1016/S0013-7944(02)00111-X)
 14. Amraei M, Skriko T, Bjrk T, Zhao X-L (2016) Plastic strain characteristics of butt-welded ultra-high strength steel (UHSS). *Thin-Walled Struct* 109:227–241. <https://doi.org/10.1016/j.tws.2016.09.024>
 15. NN: Optim mc structural steel. Ruukki. <http://www.ruukki.com/Steel/Hot-rolled-steels/Structural-steels/Optim-MC-structural-steel>. Accessed 3 Feb 2016
 16. Bono JT, DuPont JN, Jain D, Baik S-I, Seidman DN (2015) Investigation of strength recovery in welds of nucu-140 steel through multipass welding and isothermal post-weld heat treatments. *Metall Mater Trans A* 46(11):5158–5170. <https://doi.org/10.1007/s11661-015-3087-x>
 17. Xie H, Du L-X, Hu J, Sun G-S, Wu H-Y, Misra R (2015) Effect of thermo-mechanical cycling on the microstructure and toughness in the weld CGHAZ of a novel high strength low carbon steel. *Mater Sci Eng A* 639:482–488. <https://doi.org/10.1016/j.msea.2015.05.033>
 18. R.L. Brockenbrough Associates, INC. (1995) Effect of yield-tensile ratio on structural behavior—high performance steels for bridge construction. Steel Market Development Institute. <http://www.smdisteel.org/~media/Files/SMDI/Construction/Bridges%20-%20HPS%20-%20Report%20-%20Effect%20of%20Yield%20Tensile%20Ratio%20on%20Structural%20Behavior%20-%202006-06-1995.pdf>. Accessed 1 June 2017
 19. Bannister A (1999) Yield stress/tensile stress ratio results of experimental programme. FITNET. http://www.eurofitnet.org/sintap_BRITISH_STEEL_BS-25.pdf. Accessed 1 June 2017
 20. Singh SB, Bhadeshia HKDH (1998) Estimation of bainite plate-thickness in low-alloy steels. *Mater Sci Eng A* 245(1):72–79. [https://doi.org/10.1016/S0921-5093\(97\)00701-6](https://doi.org/10.1016/S0921-5093(97)00701-6)
 21. Krauss G (2015) *Steels: Processing, Structure, and performance*, second edition. ASM International, Ohio
 22. Guo B, Fan L, Wang Q, et al. (2016) The Role of the Bainitic Packet in Control of Impact Toughness in a Simulated CGHAZ of X90 Pipeline Steel. *Metals* 6:256. <https://doi.org/10.3390/met6110256>